# Urban stormwater microplastic size distribution and impact of

# subsampling on polymer diversity

- 3 Authors Swaraj Parmar, Georgia Arbuckle-Keil, G. Kumi, N.L. Fahrenfeld<sup>2\*</sup>
- <sup>1</sup>Department of Chemistry, Rutgers Camden, 315 Penn St., Camden, NJ 08102, 856-225-6333
- 5 <sup>2</sup>Civil & Environmental Engineering, Rutgers, The State University of New Jersey, 500 Bartholomew Rd,
- 6 Piscataway, NJ 08854, 848-445-8416, <u>nfahrenf@rutgers.edu</u>

#### 7 ABSTRACT

1

2

8

9

10

11

12

13

14

15

16

17

18

19

20

21

22

Understanding not only microplastic (MP) concentration but also size distribution, morphology, and polymer profiles is desirable for stormwater, which is an important pathway of entry for MP into the aquatic environment. A challenge is that subsampling is often required for analysis of environmental samples and the impact of subsampling on the stormwater MP concentration determined and the polymer types identified is poorly characterized. To address this, MP were extracted from urban, suburban, and green infrastructure stormwater. Fourier Transform Infrared microscopy was performed to characterize MP, in addition particle dimensions and morphology were recorded. Varying the number of 63-250 µm particles subsampled per sample demonstrated the coefficient of variation for concentration (standard deviation/mean) for most samples was <0.3 when 20 particles (0.8-15% of total particles) or <0.2 when 30 particles (1.2-24% of total particles) per sample were analyzed. MP concentrations in the 63-250 µm size class ranged from 15 to 303 MP/L, one to two orders of magnitude greater than observed in previously reported paired samples from the 250-500 or 500-2000 µm size classes. A total of 25 plastic polymer types were observed across samples, more than observed in the large size classes. Spectral signatures of surface oxidation indicative of weathering were observed on most

- polyethylene, polypropylene, and polystyrene particles, which were the most abundant polymer types. Fragments were the dominant morphology with average maximum length of  $158 \pm 92 \mu m$ . Overall, these results may help inform subsampling methods and be useful in future exposure assessments for aquatic organisms or design of MP removal technologies for urban and suburban stormwater.
- **KEYWORDS:** FTIR microscopy; microplastic; subsampling; oxidized polymers

# Introduction

- There is an urgent need to understand and control the pathways of entry for plastics into the water environment given estimates that 4.8–12.7 MMT of plastic litter enters the ocean each year. Microplastics (MPs) are synthetic polymers <5 mm and the majority of aquatic MPs observed in the environment result from the fragmentation of larger plastic debris. Physical and chemical (e.g., UV-degradation, oxidation, and hydrolysis) processes can both contribute to plastic fragmentation. The resulting smaller size MPs may pose a greater threat to marine biota due to the particles' resemblance to smaller size prey, increasing the chances of ingestion. Processes and translocation from the digestive tract to other tissues (for MP <83µm, as reviewed by5).
- Stormwater is a significant pathway of entry for MP pollution into the freshwater environment.<sup>6-11</sup> In addition to runoff, wet deposition of atmospheric MP can contribute to the number of MP present in stormwater.<sup>12, 13</sup> For example, -it was estimated that 62% of MPs in the Baltic Sea originates from stormwater.<sup>14</sup> Also of concern are combined sewer overflows (CSOs) that carry untreated wastewater in addition to stormwater in cities with outdated infrastructure.<sup>7, 15, 16</sup> One sampling location for the present study is among the ~700 communities in the US that have

combined sewer infrastructure.<sup>17</sup> In recent years, MP observations in stormwater have been reported from around the world (Table 1) using a range of sample volumes, techniques for extraction, and analytical approaches. Cross-study comparison is complicated by the variety of approaches applied in these studies (Table 1). Nonetheless, these studies indicate that MPs are present in stormwater and retention basins and that green infrastructure may contribute to its removal. Also, differences in land use result in varying MP sources, MP concentrations, and polymer profiles, as recently reviewed. 18 The present study builds upon previous work by our team that (1) showed higher MP concentration in stormwater compared to wastewater effluent and hydraulically connected surface waters<sup>19</sup> and (2) the influence of rainfall depth/sampling site on inter-storm variation of MP concentrations in the 250–2000 um particle size-class.<sup>20</sup> Given that the number of particles remaining after extraction from many water matrices can exceed the quantity that can be readily analyzed particle-by-particle, many researchers perform subsampling using varying number of percentages of particles to provide a representative result (Table 1). Some researchers performed chemical confirmation of visually identified particles<sup>6, 7,</sup> <sup>16, 21-23</sup> representing an improvement for preventing false positives<sup>24</sup> over visual identification alone. Others report analysis of percentages ranging from 8-10% of a sample<sup>22, 25</sup> to <1-70% or more of filter area. 10, 26 Sub-sampling techniques have been explored indicating the need to consider extraction-specific characteristics (i.e., particle distribution over a filter when performing subsampling scans of a filter<sup>27</sup>) and matrix specific characteristics (i.e., matrix-tomatrix MP concentration differences, need for more subsampling when MP concentrations are a smaller proportion of total particles in a sample<sup>28, 29</sup>). Guidance based on analysis of the impact of the number/percentage of particles subsampled would be useful not only to understand MP concentration<sup>28</sup> but also polymer diversity; the latter is also explored here.

45

46

47

48

49

50

51

52

53

54

55

56

57

58

59

60

61

62

63

64

65

66

**Table 1** Summary of stormwater MP literature including location, methods (sampling, extraction, density separation, and analysis), target particle size range, and high and low MP concentrations reported. WPO= wet peroxide oxidation, VID=visually identified, nr=not reported. Citations grouped by continent the study was from (North America, Asia, Australia, Europe) then in alphabetical order by first author

Citation	n in alphabetic Location	Volume	Extraction	Density	Analytical method,	Particle	MP conc. (MP/L)Min Max	
number		sampled (L)		separation	percent of particles on filter or number of particles analyzed	size (μm)		
This work, 19, 20	New Jersey, USA	5	WPO	NaCl	ATR-FTIR, all; microFTIR, 40 particles/sample	63- 2000	14	354
Werbowski et al. <sup>11</sup>	San Francisco, CA, USA	25-295	nr	CaCl <sub>2</sub>	FTIR, Raman, Py-GC/MS, 895 particles total	125- 1000	1.1	25
Grbic et al. <sup>22</sup>	Toronto, Canada	4	nr	CaCl <sub>2</sub>	Raman, 10% of particles	25 to ns		13
Ross et al. <sup>23</sup>	Calgary, Canada	10	WPO	Nr	Raman, 10% of VID particles	37 to >1000	<1	204
Smyth et al. <sup>6</sup>	Vaughan, Canada	0.5-2.6	nr	CaCl <sub>2</sub>	FTIR, Raman, 10% VID particles	106 to >1000	22	705
Pinon- Colon et al. <sup>7</sup>	Tijuana, Mexico	3	nr	NaCl	ATR-FTIR, percent of VID particles		66	191
Cho et al. <sup>10</sup>	Gumi, South Korea	6	WPO	Li <sub>2</sub> WO <sub>4</sub>	microFTIR, <1% of filter area	20- 5000	56	639
Sang et al. <sup>21</sup>	Wuhan, China	8	WPO	Nr	Raman, 96 VID particles	37- 5000	2.7	195
Mak et al. <sup>30</sup>	Hong Kong	192	nr	Nr	FTIR, Raman	54- 1000	1.2	6.8
Herath et al. <sup>31</sup>	New South Wales, Australia	30	WPO	NaCl	ATR-FTIR, all	48.5- 5000	1.9	2.5
Monira et al. <sup>32</sup>	Melbourne, Australia	nr	WPO	Nr	ATR-FTIR, all	15- 4600	15	33
Ziajahromi et al. <sup>16</sup>	Gold Coast, Australia	10	WPO	NaI	FTIR, >50% VID particles	25 to >500	<1	680
Lange et al. <sup>33</sup>	Vasternorrland, Sweden	<1	WPO	Nr	FTIR, microFTIR, 20-100 all		<1	8580
Liu et al. <sup>25</sup>	North of Jutland, Denmark	722- 1139	WPO	ZnCl <sub>2</sub>	FTIR, 8% sample volume	10- 2000	<1	42
Treilles et al. <sup>26</sup>	Paris, France	82-103	WPO (selected)	NaI (selected)	ATR-FTIR, 4microFTIR, all or up to 70% of filter	25- 5000	12	133

The objectives of the present study were to (1) expand our understanding of the impact of the number/percentage of particles subsampled on stormwater MP concentration and polymer types and (2) to provide new data on stormwater MP concentration size, morphology, and polymer type for previously unanalyzed particles in the 63-250 µm size class.<sup>19, 20</sup> FTIR microscopy was used to document the morphology, size, and polymer types of MP observed in stormwater.

Bootstrap analysis was applied to determine the impact of subsampling particles on the estimated MP concentration and number of total and synthetic polymer types observed. Results were then compared between sampling sites and storm events as well as to previously reported data from the larger size classes of MP.<sup>19, 20</sup> Overall, these results may help inform subsampling methods for urban stormwater and the data presented may be useful in future exposure assessments for aquatic organisms or design of MP removal technologies for urban and suburban stormwater.

## **Materials & Methods**

## Stormwater collection and MP extraction

Composite stormwater sampling (5 L total, 1 L taken every 10 to 45 min) was conducted at various urban and suburban locations in New Jersey, USA (Fig. S1). The stormwater samples analyzed in this study include three described in Bailey et al., <sup>19</sup> nine described in Boni et al., <sup>20</sup> and one not previously reported (Table 2). Samples were stored in triple rinsed 1 L glass jars (Ball Corp. Broomfield, CO) at 4°C until sieving (63-250, 250-500, 500-2000 µm). A wet peroxide oxidation was performed (20 mL 30% hydrogen peroxide with 20 mL of 0.05 M FeSO<sub>4</sub>, heated on a hot plate at 65°C and stirred at 120 rpm for at least 30 minutes). <sup>31</sup> Then, samples were suspended in a saturated NaCl solution in glass funnels with surgical tubing clamped at the outlet. Funnels were topped with foil to prevent contamination, and allowed to sit overnight

after which settled particles were emptied through the surgical tubing. <sup>31</sup> Positively buoyant particles ( $\rho$  < 1.2 g/cm<sup>3</sup>) were filtered onto stainless steel mesh (20 µm, TWP, Berkeley, CA) and stored in closed glass petri dishes until analysis. For quality assurance and control, field blanks (two from Bailey et al., <sup>19</sup> one from Boni et al. <sup>20</sup>) consisting of 1 L deionized or tap water were analyzed in parallel with the field samples. Note, future studies should consider the now available American Society for Testing and Materials (ASTM) methods <sup>34</sup> that recommend sample volume, adding digestions to reduce non-plastic debris (e.g., cellulose degradation), and facilitate capture of non-buoyant particles by not performing density separation (which would include most tire-wear). Field blanks and matrix spike (MS) recoveries were performed as described previously with MS recovery of 97% ± 6% for known quantities of polyethylene extracted from a personal care product in the 250-2000 µm size range. <sup>20</sup>

# Subsampling

The substantial number of particles present in the 63-250 μm size class (Table 2) made analyzing all particles using the methods applied here infeasible. Therefore, all particles were counted in each sample and the subset of particles analyzed were scaled to estimate total MP concentrations (Eq 1). For counting total particles, images were taken of the particles on the filters (47 mm diameter) using a Moticam<sup>TM</sup> 580 microscope camera (Motic Asia, Hong Kong); particles were manually counted using ImageJ<sup>TM</sup> (https://imagej.nih.gov/ij/). To aid the counting process, a sample petri dish was placed on a pattern which consisted of 21 circular numbered segments (Fig. S2). A 1951 USAF resolution test chart (Edmund Optics, Barrington, NJ) was used to determine which particles were smaller than 62.50 μm (in all dimensions, Fig. S3) and these particles were excluded from the total particle count (as the focus was on the 63-250 μm size range particles).

To facilitate the subsampling of particles on a filter, given that particles appeared relatively evenly distributed across the filter (Fig. S4), a pie cut stencil was created with eight equal sectors that was then divided into twenty numbered sections (Fig. S5). Note, recommendations regarding the schema used for subsampling have been explored by other researchers and careful consideration of particle distribution patterns should be considered prior to subsampling. A random number generator was used to determine which of the twenty sections to sample from, with two particles in the center of the respective section selected for analysis followed by rotating the filter 45° counterclockwise to allow sampling from one of the twenty sections of the adjacent pie slice sector of the filter. The process was repeated until 40 particles per sample were collected for FTIR analysis. This number of particles was selected following bootstrap analysis of FTIR analysis results from 81 particles from Field P (10/12/2020), described below. Across the stormwater samples, a total of 521 particles were analyzed, representing 1.6-31% of total particles per sample (Table 2).

# Vibrational spectroscopy

Identification of stormwater MPs was conducted primarily via a Bruker LUMOS FTIR-microscope which utilizes a liquid nitrogen cooled MCT detector (Bruker Optics, Ettlingen, Germany). Due to their small size, selected particles were transferred onto an IR substrate using needles (Coats and Clark, Charlotte, NC). A visual image of the particle was taken, allowing for the length to be measured, morphology (fiber, rods, fragments, films, spheres) to be identified, and color to be recorded (examples of each morphology are provided in Fig. S7). For data collected in reflectance mode, particles were placed onto Mirr IR slides (Kevley Tech., Chesterland, OH). For FTIR transmission data, particles were transferred onto a CaF<sub>2</sub> disc (size: 32 mm × 3 mm) (International Crystal Laboratories, Garfield, New Jersey). An aperture of 10

μm × 10 μm for both background (64 scans of IR substrate) and sample scans (32-64 scans) and a 4 cm<sup>-1</sup> resolution provided acceptable spectra for this study. For black rubbery particles that gave poor quality spectra on the LUMOS 1 microscope, analysis was repeated using an Alpha<sup>TM</sup> FTIR-ATR Spectrometer (Bruker Optics, Billerica, MA) with a diamond IRE and Deuterated Triglycine Sulfate (DTGS) detector. Background scans of air were collected (64 scans, to provide the spectral background), and suspected rubber particles were transferred onto the IRE crystal using metal tweezers. To be consistent with parameters used on the LUMOS, 32-64 sample scans were collected. If quality spectra could not be obtained via FTIR, analysis was performed via Raman microscopy (XploRA Plus, Horiba, Piscataway, New Jersey). After calibration with a silicon standard, particles were relocated onto a glass slide and placed on the Raman stage. The 10x and 50x objectives were used to collect visual images and focus on the surface of the sample and 50x and 100x were primarily used for spectral acquisition.

# Spectral Analysis

Spectra were interpreted by identifying major bands and by comparison with known polymer spectra. Based on the wavenumber, relative intensity, and shape of the major bands, the identity of each particle was determined. For simple spectra of well-known polymers, e.g., polyethylene, polypropylene, or polystyrene with little to no weathering effects, no database search was necessary, and the MP particle was identified as the respective polymer. Otherwise, the polymer library from OPUS software (Version 7.2), siMPle<sup>TM</sup> (version 1.1.β),<sup>35-37</sup> and/or OpenSpecy<sup>TM</sup> (https://openanalysis.org/openspecy/)<sup>38</sup> were searched for matches based upon hit quality. Consistency of database matches was considered as well as visual inspection of spectral matches.

#### Statistical Analysis

The data collected from this study were evaluated using statistical analysis in Rstudio (www.project-r.org). To estimate the total 63-250 µm microplastic concentration in each stormwater sample ([MP]<sub>est</sub>, MP/L), the number of microplastics observed in each 40-particle subsample (N<sub>MP</sub>) was scaled assuming the percentage of MP in the subsample was similar to the total number of particles in the sample:

$$[MP]_{est} = \frac{N_{MP}}{40 \text{ particles}} \times \frac{Total \text{ particles}}{Volume \text{ of sample}} \text{ Eq } 1$$

A Shapiro-Wilk normality test confirmed the non-normality of the MP concentration data across sampling sites. Random forest (randomForest package) was used to evaluate the impact of factors (i.e., site, rainfall, antecedent dry days) on MP concentrations. To compare polymer profiles across collection sites and sieve size classes, polymer concentrations were log-transformed and a Bray-Curtis dissimilarity matrix was created for use in ordination and represented via non-metric multidimensional scaling (nMDS). An analysis of similarities (i.e., *Table 2 Details of sampling events: sampling site, date of sampling, cumulative rainfall measured in cm, antecedent dry days prior to storm event (data from https://www.ncdc.noaa.gov/cdo-web/), and total particles (MP and non-MP).* 

Site	Description	Date (m/d/y)	Cumulative rainfall (cm)	Antecedent dry days	Total particles (63-20 μm)	Citation (if previously reported)
City N	End of pipe, urban area and heavily trafficked highway	10/16/2019	3.05	9	275	16
					(Field blank 41)	
		8/4/2020	4.01	3	737	17
		10/12/2020	3.00	11	290	17
		10/29/2020	4.50	12	672	17
Field P	End of pipe, suburban college campus, adjacent to sports fields with artificial turf	10/16/2019	3.05	9	704	16
					(Field Blank 160)	
		8/4/2020	4.01	3	925	17
		10/12/2020	3.00	11	175	17
		10/29/2020	4.50	12	202	17
		8/17/2020	1.50	4	2521	17

Bio-	Overflow pipe,	8/19/2020	1.88	1	2021	17
retention	located on suburban				(Field blank 74)	
P	college campus next					
	to parking lot, road,					
	and buildings					
City B	In-pipe, combined	10/16/2019	5.41	4	404	16
	sewer*					
City K	End of pipe, urban	12/10/2019	3.78	5	127	
	area					

<sup>\*</sup>sampling conducted with an autosampler during CSO event; all other sampling by hand

ANOSIM) test was performed on the dissimilarity matrix to understand if size class and collection site were factors associated with the polymer profiles observed.

## Results

### Particle count and subsampling

Subsampling of particles prior to chemical analysis was required due to the large number of particles remaining after extraction and density separation. Total particles in 63-250 µm size range after extraction had a median of 538 particles per 5L of stormwater sampled (Table 2). Field blanks had significantly less particles than the stormwater samples (p=0.0088, Wilcoxon rank sum), with a median of 74 particles per sample (Table 2). To determine the number of particles that can be subsampled and give reliable representation of the MP concentration, 81 particles were randomly subsampled from Field P 10/12/2020 (which had a total particle count of 175 particles). Out of the 81 randomly selected particles, 43 were identified to be MPs, the remaining particles were either non-plastic (e.g., plant matter, natural fibers) or spectra that could not be identified. Eighteen materials were identified of which 15 were plastics, out of the 81 particles analyzed. Bootstrap analysis indicated that subsampling 5, 10, 20, 40, or 50 particles and scaling (Eq 1) to estimate total MP concentration resulted in a relative percent difference from analyzing all 81 particles of 18±11, 19±22, 20±10, 4.7±3.3%, 3.6±2.8% RPD (N=5),

respectively. Subsampling 5, 10, 20, 30, 40, or 50 particles resulted in  $4.0\pm0.7$ ,  $6.8\pm0.8$ ,  $9.0\pm1.0$ ,  $13.6\pm1.1$ , and  $15\pm0.7$  unique polymer types, respectively, of which  $2.2\pm0.4$ ,  $3.8\pm1.3$ ,  $5.6\pm0.9$ , 9.6±1.1, and 11±0.8 were plastics. Based on these results and practicality, subsampling of stormwater samples was performed for 40 particles to reduce error on MP concentration estimations and understand the diversity of polymer types in a given sample. Subsampling the selected 40 particles/sample resulted in analysis of 11.4±9.3% of particles/sample (range: 1.6 to 31.5% of total particles, total particle counts listed in Table 2). The bootstrap analysis was repeated on the other samples subsampling 5, 10, 20, or 30 particles to create (1) covariance plots for MP concentration (standard deviation/mean) at different sampling depths and (2) polymer rarefaction curves (number of unique polymer types versus number of particles subsampled). The latter provides visual representation of whether the sampling depth likely captured most polymer types in a given sample (Fig. 1). This indicates that subsampling 40 particles underestimates the plastic diversity in some samples (e.g., BBR 8/17/2020, City N 10/16/2019) while in others, subsampling as few as 20 particles in our samples was sufficient to capture the diversity observed by subsampling 40 particles (e.g., City K 12/10/2019, Field P 10/16/2019).

197

198

199

200

201

202

203

204

205

206

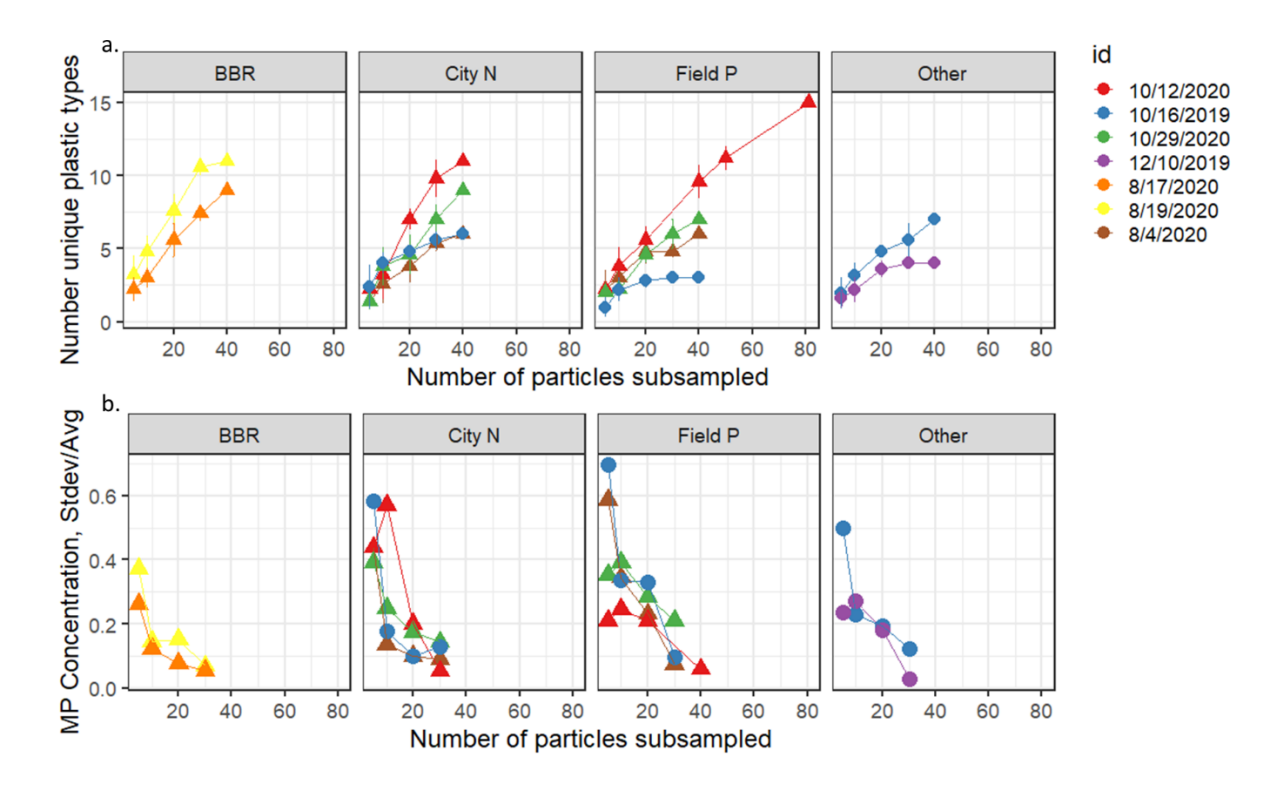
207

208

209

210

211



213

214

225

Fig. 1 a. Material rarefaction curves showing the number of unique materials versus the number 215 of particles subsampled (top) and **b**. coefficient of variation (standard deviation/average) for 216 extrapolated MP concentrations as a function of the number of particles subsampled (replication N=5). The colors correspond to different storm events (date) and shape to sampling year 217 218 (triangles for 2020, circles for 2019). City K and City B included under "Other." 219 Microplastic polymer types, concentrations, morphologies, and size distributions 220 A total of 521 particles were analyzed via FTIR-microscopy. Microplastics were observed at 221 each of the five sampling sites for the 63-250 µm size class, resulting in observations of 24 222 plastic polymer types across the samples (Fig. 2). Major commercial polymers such as 223 polyethylene (PE), polypropylene (PP), and polystyrene (PS) were detected at each sampling 224 site. Other polymer types prevalent in stormwater were polyamide (PA), ethylene-propylene

copolymer (EPDM), rayon, and acrylic MPs (example spectra are shown in Fig. S6).

MP concentrations for the 63-250  $\mu$ m size class ranged from 15 MP/L at City K to 303 (±50) MP/L in Bioretention P effluent. MP concentrations in 63–250 µm size class were one to two orders of magnitude greater than those previously reported for 250-500 µm and 500-2000 µm size classes for these samples (both p=0.015, posthoc pairwise t-test with Bonferroni correction). 19, 20 Random forest indicated that 60.8% of the variance in the concentration in the 63-250µm size class was explained by antecedent dry days (10.3% increase in mean square error MSE) followed by site and rainfall depth (7.4 and 5.6% increase in MSE, respectively). Blanks taken at Field P, City N, and City B had MP particles present: Field P blank had 56 MP, City N had 8 MP, and City B had 30 MP. The reported stormwater MP concentrations were not corrected for the contamination observed in the field blanks given that the field blanks were 1 L water samples rather than 5 L as for the stormwater samples. The blanks (which only contained PE and PP) had 6.3-57 times less MP per filter than storm samples (p= 0.0044, Wilcoxon rank sum). Fragments were the most commonly observed morphology for MP for all polymer types (Fig. 3) and sampling sites. Film and rods were the next most observed morphologies while beads were rarely observed in these samples (examples are shown in Fig. S7). Examples of all morphologies observed are shown in Fig. S7. Histograms of the minimum measured dimension across particle morphologies indicated that data were generally right skewed, and the tail illustrated that some particles larger than expected for this sieve size were observed. These minimum dimensions measured however do not capture all three dimensions and for example the PA rod's diameter likely allowed it to pass through the 250 µm sieve opening.

226

227

228

229

230

231

232

233

234

235

236

237

238

239

240

241

242

243

244

245

Polymer profiles differed by size class rather than by sampling site (p=0.001 and 0.55, respectively, ANOSIM) when including the data collected in this study and the previously reported larger MP. Some clustering within the 63 – 250 μm size class was observed by sample site, with Field P separated from BBR and City N, and City N but with overlap for all with City N (Fig. 4). A similar pattern is seen for the larger two MP size classes within their cluster.

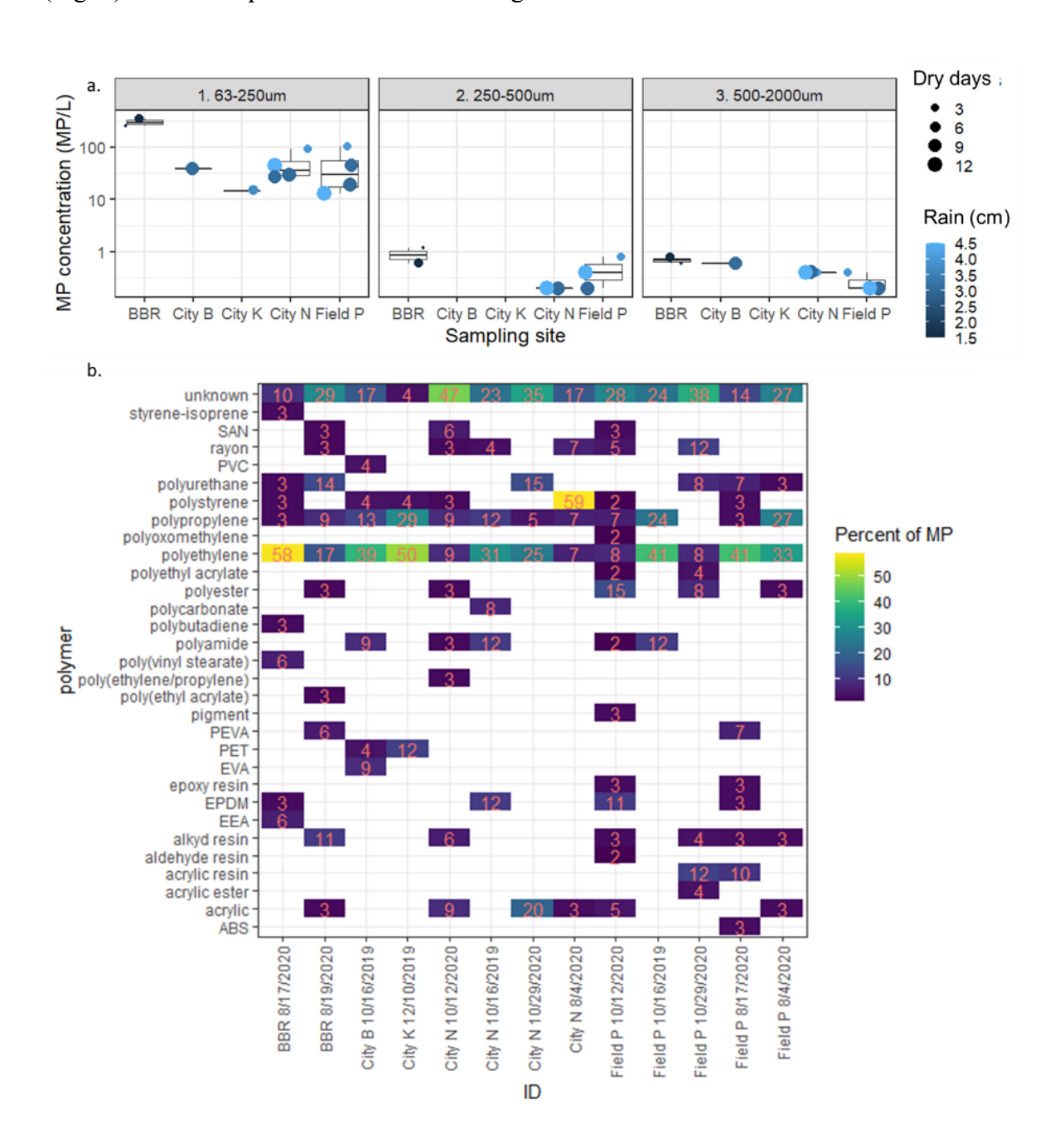


Figure 2 a. Boxplots of MP concentrations (MP particles per liter of water) observed in the bioretention basin and stormwater at each sampling site: City N, City B, City K, Bioretention Basin (BBR), and Field P. For each respective size class 63-250 µm, 250-500 µm and 500-2000 µm. Circle color represents cumulative rainfall in cm and size represents antecedent dry days. The two larger size classes show data from Boni et al. and Bailey et al. b. Heatmap of polymer profile distribution observed across sampling sites and events. BBR represents Bioretention P. Polymer abbreviations: SAN is Styrene-Acrylonitrile copolymer, PVC is Polyvinyl Chloride, PU is Polyurethane, PS is Polystyrene, PP is Polypropylene, PEVA is Polyethylene Vinyl Acetate, PET is Polyethylene Terephthalate, PEA is Polyethyl Acrylate, PE is Polyethylene, PB is Polybutadiene, PA is Polyamide, EPDM is a Poly(Ethylene-Propylene) copolymer, EEA is Ethylene-Ethyl-Acrylate copolymer, ASA is Acrylonitrile Styrene Acrylate copolymer, and ABS represents Acrylonitrile Butadiene Styrene copolymer. (Example spectra are available in the Appendix, note butadiene polymer spectra were obtained with ATR-FTIR.)

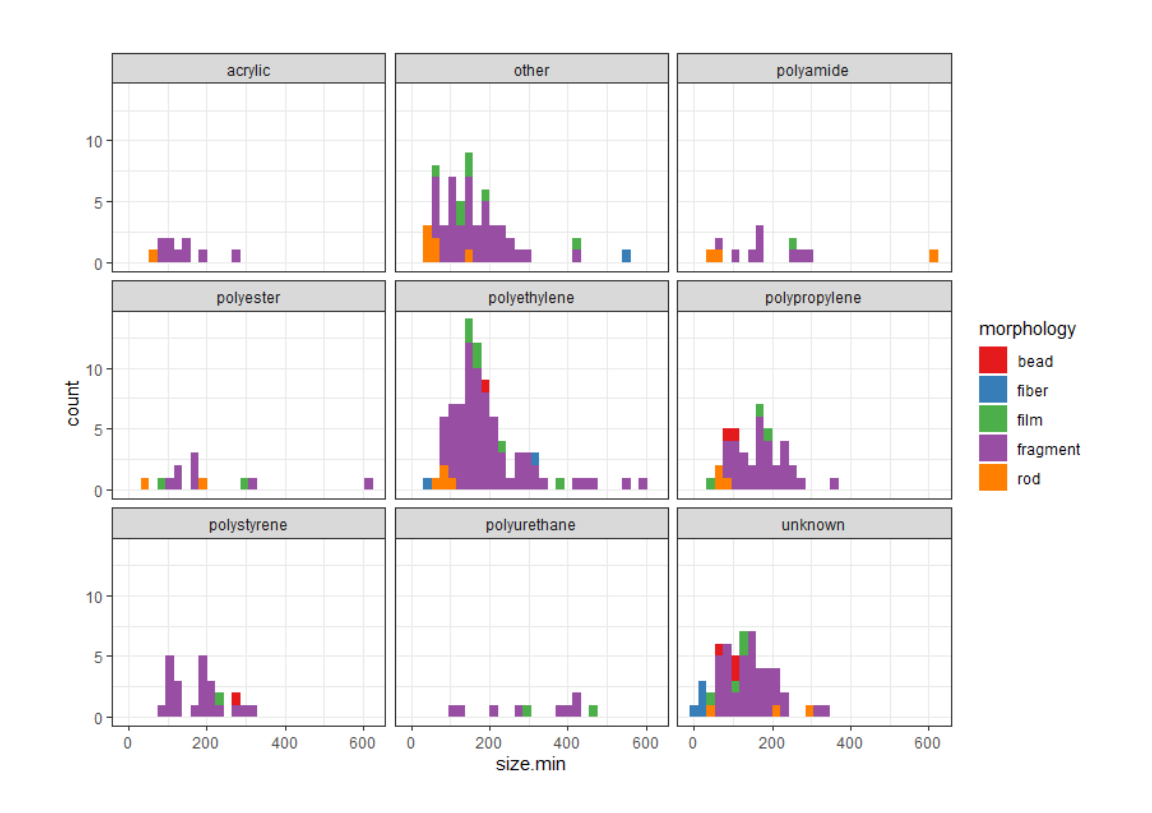
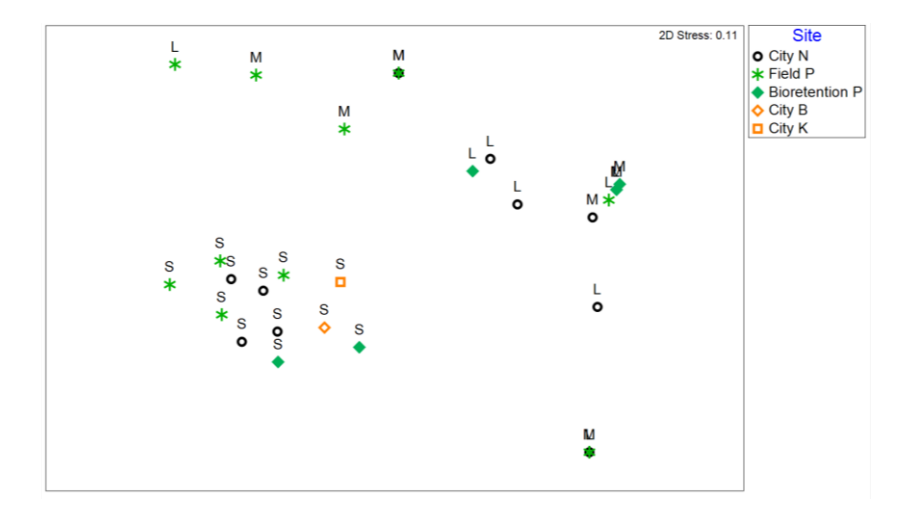


Figure 3: Histograms of measured particle length (minimum dimension measured) as a function of polymer material with color corresponding to the observed particle morphology. Other includes microplastics present at lower prevalence in the samples and does not include unknown or natural materials observed.



**Fig. 4** nMDS of log-10 transformed polymer profiles. Symbols correspond to different sampling locations (site). The letter above each symbol indicates the size range: S for 63-250 μm, M for 250-500 μm, and L for 500-2000μm.

## Discussion

## Subsampling

The sample matrix/volume sampled and extraction methods applied here (wet peroxide oxidation and density separation) resulted in too many particles to analyze in the 63-250 µm size range via manual FTIR microscopy. This was partly due to the presence of non-plastic particles including materials identified via FTIR as natural fibers, plant matter, clay, sand, and cellulose. Notably, applying a cellulose digestion (e.g., using modified Schweizer's reagent via ASTM Method

8333-20<sup>34</sup> or enzyme digestion via cellulase<sup>39</sup>) could help reduce the number of non-plastic 282 particles remaining identified as cellulose. Cellulose was observed in nine of the twelve samples 283 284 analyzed and when observed it accounted for 7.3±6.1% (range of 2.5 to 20%) of particles 285 analyzed. 286 The percentage of particles to analyze was explored given that there is not a consensus in the 287 literature for subsampling stormwater (Table 1). Random sampling rather than analysis of only visually identified particles was pursued given reports that visual identification can over- or 288 underestimate microplastic concentration,<sup>24</sup> as particles without vibrant colors may be missed. 289 290 Here, the subsampling pattern was selected after visual inspection of the filters, as others have 291 suggested the particle distribution should be considered prior to subsampling for methods with scans of filter area.<sup>27</sup> Subsampling patterns with randomly selected particles were not previously 292 shown to vary by the sampling pattern selected (cross, spiral, etc.).<sup>28</sup> 293 294 The number of subsampled particles to accurately estimate MP concentrations has been 295 investigated, however the sample matrix and preparation should be considered when comparing across studies. For example, a study<sup>27</sup> of surface water, wastewater, and rainwater particles 296 297 washed with ethanol reported that subsampling 50% of particles would result in error of 20%. 298 However, those authors note decreasing error for subsampling with increasing MP content, and 299 the oxidation or density separation performed in the present study helps reduce debris prior to 300 filtration. Another team recommended subsampling at least 30 particles >100 µm extracted from 301 surface water, stormwater, and sediment to accurately estimate MP concentrations (i.e., error 302 <20%), noting that the portion of MP in a sample was more important than the total particle count.<sup>29</sup> The selection of 40 particles/sample here represents up to 31.5% of sample particles and 303

given the focus on particles in a smaller size range is not surprisingly higher than previously suggested.

Further subsampling of Field P 10/12/2020 is expected to result in more plastic types being observed given that the polymer rarefaction curves have not reached asymptote even at 50% sampling depth (N=81 particles). However, the leveling of the polymer rarefaction curves for the same site when sampled on 10/16/2019 indicates temporal variation in the subsampling required. Of course, these analyses are based upon the polymer classes reported here, which in themselves contain spectra with varying amounts of oxidation. Researchers should also consider the study aim when subsampling is needed for analysis because the subsampling coverage for consistent estimates of total MP concentration may be insufficient for describing polymer diversity. Reporting the concentration of specific polymer types may be desirable rather than total MP knowing that the polymers and their associated plasticizers, additives, and dyes have varying properties<sup>40</sup> and the ecological impacts could be polymer-target specific (e.g., demonstrated impact of tire rubber (leaching of anti-oxidant) to coho salmon<sup>41</sup>).

Observed MP concentrations, sizes, and morphologies

MP concentrations for the 63-250 μm size class were significantly larger when compared to concentrations for 250-500 μm and 500-2000 μm for paired samples. <sup>19, 20</sup> Higher concentrations of MP in smaller size classes are consistently reported across water matrices, <sup>42</sup> likely due to particle counts increasing as plastics fragment. Direct comparisons to other studies are complicated by the varying sample volumes, extraction techniques, analytical techniques, target size ranges <sup>18, 42</sup> as described in the introduction, in addition to likely geographic and temporal differences. Nonetheless, the maximum concentration observed here were within an order of

magnitude of the maximum concentrations reported in several studies. 6, 7, 21, 26, 43 One order of magnitude lower maximum concentrations were reported by some studies, potentially due to those researchers looking at smaller size ranges 11, 22, 30 or differences in sample volume. 30, 44, 45 Researchers in Sweden that reported an order of higher maximum MP concentration in stormwater notably included particle sizes smaller than examined here, down to 20 µm. <sup>33</sup> Including smaller particle sizes is recommended in future studies but is impractical to do using the methods applied here given the labor required and the analytical limitations. Antecedent dry days followed by rainfall depth and sampling site were factors associated with MP concentrations here, similar to our previous study of the larger MP which indicated these same factors; rainfall and sampling site exhibited greater mean square error than antecedent dry days.<sup>20</sup> Similarly, a relationship between antecedent dry days and MP concentrations was reported from a study in Mexico, albeit with longer dry periods (c.a. months) before storm events. Site-to-site differences were expected due to differences in land use and land cover, also reported in other catchments, <sup>10, 23</sup> as well as sewer type. For example, City B samples were collected during a storm from combined sewers, whereas City N has separate sanitary sewers. Polymer morphologies were primarily fragments, similar to other stormwater studies that reported morphologies. 11, 21, 23 Fibers are also often abundant in stormwater including that from CSOs, <sup>7, 11</sup> but this morphology was not especially prevalent for the MP observed here including from the CSO event sampled for City B. Polymer minimum dimensions provided here demonstrated observations of some particles not within the expected size class based on the two dimensions measured. This is likely partly due to the presence, for example, of rods with small enough diameter to pass through the sieves

326

327

328

329

330

331

332

333

334

335

336

337

338

339

340

341

342

343

344

345

346

(diameter dimension was not measured) or films whose flexibility may allow passage. Other factors may include irregularities in the sieves or contamination which is more likely for smaller particles (notably, PE and PP were the only MP observed in blanks). Reporting actual particle size in addition to size classes can aid in cross-study comparison. The recommendation to measure particle size is being incorporated into an emerging standard method<sup>46</sup> and remains of interest given that different standard methods are suggesting different sieve sizes. <sup>34, 46</sup> Understanding particle size and morphology may aid in design of treatment systems (if removal of MP is desirable) and inform ecological exposure assessment, as different particle sizes and morphologies may appeal to different aquatic organisms. Likewise, different morphologies have different translocation/stress induction potential as reviewed by 5 and fate given the different bivalve egestion rates for spheres versus fibers.<sup>47</sup> Observations of MP present in the field blanks may be due to atmospheric deposition (field blanks were left open during sampling) and/or cross contamination in the lab. Others have reported wet deposition of MP during rainfall events. 12, 13, 48. Negligible blank contamination is commonly reported, particularly for studies looking for smaller MP: of the 14 stormwater studies included in Table 1, eleven included field and/or lab blanks in their protocols<sup>6, 7, 11, 16, 22, 23, 25, 30,</sup> <sup>33, 44</sup> and eight reported some contamination in the blanks. If not from atmospheric deposition during sampling, cross contamination in the lab or during sampling processing is possible, hence recommendations to not wear synthetic materials while sampling, working in HEPA filtered areas, as recently outlined. 46

MP polymer profiles in stormwater

348

349

350

351

352

353

354

355

356

357

358

359

360

361

362

363

364

365

366

367

The smaller size MPs analyzed here showed a greater variety of polymer types, resulting in certain polymer species found in this study that were not previously noted in the >250 µm size classes (for which only PE, PP, PS, PETE, and ABS were observed). 19,20 Examples of polymers only observed in the smaller size class (63-250 µm) include acrylic copolymers, styrene-isoprene copolymers, epoxy resins, and EPDM copolymers. The greater number of polymer types in the smaller size range may be associated with (a) the larger number of total particles such that larger sample volumes would be needed to observe these particles in the larger size ranges, (b) the greater likelihood of certain polymers to fragment into smaller sizes, and/or (c) differences in transport via stormwater and/or deposition as a function of particle size. The most prevalent polymer types (PE, PP, PS, polyamides, and acrylics) have an array of applications and are commonly observed across water matrices <sup>49</sup> including stormwater. <sup>40</sup> Several other polymers are used in bitumen applications such as roofs and pavement (e.g., styrene isoprene copolymer, polyvinyl stearate, and EEA copolymer) or tires (e.g., polybutadiene). While butadiene rubbers often do not provide good spectra via FTIR, there have been ATR-FTIR studies of ABS that were able to document spectral changes associated with photodegradation.<sup>50</sup> Here the two observed particles were analyzed via ATR-FTIR (see example spectra Fig. S6i) where we hypothesize that with these smaller particles when compressed had sufficient contact with the IRE crystal to provide quality spectra. (Notably this is likely an underestimate of ABS prevalence in our samples given that a density separation was performed during extraction, and others report rubbers to be prevalent in stormwater particularly from road runoff<sup>11</sup>). Further study would be needed to confirm the potential sources of the plastics observed, including perhaps through more extensive spectral analysis to possibly identify unique dyes, or specific copolymers, or other additives<sup>e.g.,51</sup> that may be more use specific.

369

370

371

372

373

374

375

376

377

378

379

380

381

382

383

384

385

386

387

388

389

390

Interestingly, some polymers (PVC and PC) were not expected to be observed in this study due to having higher densities than the saturated NaCl solution used for density separation (>1.202 g/mL). Newer standard methods no longer suggest density separation in order to facilitate observation of denser polymers<sup>34</sup> or researchers may apply denser salt solutions (Table 1). These denser particles may have been attached to less dense particles allowing them to bypass density separation. It is believed to be unlikely that contamination was the source of these particles because no PVC or PC polymer was found/identified in the field blanks (only PE and PP) and the samples were not exposed to PVC or PC during processing. Challenges with the spectral analysis are noted, including the influence of surface oxidation (Fig. S6) and particle thickness. In some samples this limited the ability to initially collect quality spectra in transmission mode; multiple locations per particle were analyzed to obtain spectra which could be identified as a specific polymer. Matches from spectral databases often required additional manual interpretation. Different researchers have reported using various proprietary and open spectral libraries and a range of match scores to accept and/or inspect spectra. Here, this included analyzing if there was consistency in the list of top hits as well as manual inspection of major bands to confirm identity, rather than accepting any spectral match above a

# Conclusion

certain database match score.

392

393

394

395

396

397

398

399

400

401

402

403

404

405

406

407

408

409

410

411

412

413

Results of the present study indicate that MP concentrations were one to two orders of magnitude greater in the 63-250  $\mu$ m particle size class compared to 250-500  $\mu$ m or 500-2000  $\mu$ m, previously reported. <sup>19, 20</sup> A greater number of polymer types were observed in the smaller size range, information that may be useful in future exposure assessments for aquatic organisms.

Future studies are recommended that target a wider range of particle densities and include cellulose degradation to help remove non-plastic debris. Likewise, including particles in smaller size range than was feasible here is also recommended, but is impractical to do so quantitatively using the methods applied in this study and likely requires higher throughput methods that may provide less robust particle size/morphology data. Subsampling analyses indicated that a greater diversity of polymer types is expected to be observed in samples from the same site if more particles were analyzed, again underscoring the need for subsampling designs that are study specific<sup>27, 28</sup> or analyses implementable with higher throughput, for which FPA and Raman scanning methods have been proposed. 35, 36, 52 However, higher throughput should not sacrifice the ability to accurately interpret results, as here the need for manual interpretation of many spectra from the environmental samples was noted. The polymer profiles' spatial and temporal variation at stormwater outfalls in the urban/suburban environment as well as a bioretention basin was demonstrated within the same region. These results may help inform the expected exposure to different positively buoyant polymer types in stormwater and the potential for treatment.

## Acknowledgements

414

415

416

417

418

419

420

421

422

423

424

425

426

427

428

429

430

431

432

433

434

435

This manuscript is the result of research sponsored by the National Science Foundation Grant (1917676), Water Research Foundation Project 5088, NJ Space Grant, and New Jersey Sea Grant Consortium (NJSGC) with funds from the National Oceanic and Atmospheric Administration (NOAA) Office of Sea Grant, U.S. Department of Commerce, under NOAA grant number NA18OAR170087. Thanks to Will Boni, Shreya Patil, and Kendi Bailey for stormwater sample collection and extraction.

#### 436 References

- 437 1. J. R. Jambeck, R. Geyer, C. Wilcox, T. R. Siegler, M. Perryman, A. Andrady, R. Narayan
- 438 and K. L. Law, Science, 2015, 347, 768.
- 439 2. A. L. Andrady, *Marine Pollution Bulletin*, 2011, **62**, 1596-1605.
- 440 3. A. L. Andrady, in *Marine Anthropogenic Litter*, eds. M. Bergmann, L. Gutow and M.
- Klages, Springer International Publishing, Cham, 2015, DOI: 10.1007/978-3-319-16510-
- 442 3 3, pp. 57-72.
- 443 4. L. Su, B. Nan, K. L. Hassell, N. J. Craig and V. Pettigrove, *Chemosphere*, 2019, **228**, 65-
- 444 74.
- 445 5. A. C. Mehinto, S. Coffin, A. A. Koelmans, S. M. Brander, M. Wagner, L. M. Thornton
- Hampton, A. G. Burton, E. Miller, T. Gouin, S. B. Weisberg and C. M. Rochman,
- 447 *Microplastics and Nanoplastics*, 2022, **2**, 17.
- 448 6. K. Smyth, J. Drake, Y. Li, C. Rochman, T. Van Seters and E. Passeport, *Water Research*,
- 449 2021, **191**, 116785.
- 450 7. T. d. J. Piñon-Colin, R. Rodriguez-Jimenez, E. Rogel-Hernandez, A. Alvarez-Andrade
- and F. T. Wakida, Science of The Total Environment, 2020, 704, 135411.
- 452 8. A. Gilbreath, L. McKee, I. Shimabuku, D. Lin, L. M. Werbowski, X. Zhu, J. Grbic and
- 453 C. Rochman, Journal of Sustainable Water in the Built Environment, 2019, 5, 04019004.
- 454 9. I. Järlskog, A.-M. Strömvall, K. Magnusson, M. Gustafsson, M. Polukarova, H. Galfi, M.
- 455 Aronsson and Y. Andersson-Sköld, *Science of The Total Environment*, 2020, **729**,
- 456 138950.
- 457 10. Y. Cho, W. J. Shim, S. Y. Ha, G. M. Han, M. Jang and S. H. Hong, Science of The Total
- 458 Environment, 2023, **866**, 161318.

- 459 11. L. M. Werbowski, A. N. Gilbreath, K. Munno, X. Zhu, J. Grbic, T. Wu, R. Sutton, M. D.
- Sedlak, A. D. Deshpande and C. M. Rochman, ACS ES&T Water, 2021, DOI:
- 461 10.1021/acsestwater.1c00017.
- 462 12. R. Dris, J. Gasperi, M. Saad, C. Mirande and B. Tassin, Marine Pollution Bulletin, 2016,
- **104**, 290-293.
- 464 13. Y. Zhang, S. Kang, S. Allen, D. Allen, T. Gao and M. Sillanpää, Earth-Science Reviews,
- 465 2020, **203**, 103118.
- 466 14. G. Schernewski, H. Radtke, R. Hauk, C. Baresel, M. Olshammar and S. Oberbeckmann,
- 467 *Frontiers in Marine Science*, 2021, **8**, 594415.
- 468 15. Y. Zhou, Y. Li, Z. Yan, H. Wang, H. Chen, S. Zhao, N. Zhong, Y. Cheng and K.
- 469 Acharya, Water Research, 2023, 236, 119976.
- 470 16. S. Ziajahromi, D. Drapper, A. Hornbuckle, L. Rintoul and F. D. L. Leusch, Science of
- 471 *The Total EEnvironment*, 2020, **713**, 136356.
- 472 17. U. S. Environnmental Protection Agency (EPA), Combined Sewer Overflow
- Basics(Online) Available: https://www.epa.gov/npdes/combined-sewer-overflow-basics
- 474 18. C. Stang, B. A. Mohamed and L. Y. Li, Journal of Environmental Management, 2022,
- **317**, 115510.
- 476 19. K. Bailey, K. Sipps, G. Saba, G. Arbuckle Keil, B. Chant and N. Fahrenfeld,
- 477 *Chemosphere*, 2021, **272**.
- 478 20. W. Boni, G. Arbuckle-Keil and N. L. Fahrenfeld, Science of The Total Environment,
- 479 2022, **809**, 151104.
- 480 21. W. Sang, Z. Chen, L. Mei, S. Hao, C. Zhan, W. b. Zhang, M. Li and J. Liu, Science of
- 481 *The Total Environment*, 2021, **755**, 142606.

- 482 22. J. Grbić, P. Helm, S. Athey and C. M. Rochman, *Water Research*, 2020, **174**, 115623.
- 483 23. M. S. Ross, A. Loutan, T. Groeneveld, D. Molenaar, K. Kroetch, T. Bujaczek, S. Kolter,
- S. Moon, A. Huynh and R. Khayam, Frontiers in Environmental Science, 2023, 11, 36.
- 485 24. S. Ziajahromi, P. A. Neale, L. Rintoul and F. D. L. Leusch, Water Research, 2017, 112,
- 486 93-99.
- 487 25. F. Liu, K. B. Olesen, A. R. Borregaard and J. Vollertsen, *Science of The Total*
- 488 *Environment*, 2019, **671**, 992-1000.
- 489 26. R. Treilles, J. Gasperi, A. Gallard, M. Saad, R. Dris, C. Partibane, J. Breton and B.
- 490 Tassin, *Environmental Pollution*, 2021, **287**, 117352.
- 491 27. C. Thaysen, K. Munno, L. Hermabessiere and C. M. Rochman, *Applied spectroscopy*,
- 492 2020, **74**, 976-988.
- 493 28. J. Brandt, F. Fischer, E. Kanaki, K. Enders, M. Labrenz and D. Fischer, Frontiers in
- 494 Environmental Science, 2021, 8.
- 495 29. H. De Frond, A. M. O'Brien and C. M. Rochman, *Chemosphere*, 2023, **310**, 136772.
- 496 30. C. W. Mak, Y. Y. Tsang, M. M.-L. Leung, J. K.-H. Fang and K. M. Chan, *Marine*
- *Pollution Bulletin*, 2020, **157**, 111181.
- 498 31. S. Herath, D. Hagare, Z. Siddiqui and B. Maheshwari, Environ Monit Assess, 2022, 194,
- 499 173.
- 500 32. S. Monira, R. Roychand, M. A. Bhuiyan, F. I. Hai and B. K. Pramanik, *Chemosphere*,
- 501 2022, **299**, 134389.
- 502 33. K. Lange, K. Magnusson, M. Viklander and G. T. Blecken, Water Res, 2021, 202,
- 503 117457.

- 504 34. ASTM 8333, Standard Practice for Preparation of Water Samples with High, Medium,
- or Low Suspended Solids for Identification and Quantification of Microplastic Particles
- and Fibers Using Raman Spectroscopy, IR Spectroscopy, or Pyrolysis-GC/MS, 2021.
- 507 35. S. Primpke, P. Dias and G. Gerdts, *Analytical Methods*, 2019, **11**, 2138-2147.
- 508 36. S. Primpke, C. Lorenz, R. Rascher-Friesenhausen and G. Gerdts, *Analytical Methods*,
- 509 2017, **9**, 1499-1511.
- 510 37. S. Primpke, M. Wirth, C. Lorenz and G. Gerdts, *Analytical and Bioanalytical Chemistry*,
- **2018**, **410**, 5131-5141.
- 512 38. W. Cowger, A. Gray, H. Hapich, C. Rochman, J. Lynch, S. Primpke, K. Munno, H. De
- Frond and H. O., Open Specy. (Online) Available: www.openspecy.org. 2020.
- 514 39. M. G. J. Löder, H. K. Imhof, M. Ladehoff, L. A. Löschel, C. Lorenz, S. Mintenig, S.
- Piehl, S. Primpke, I. Schrank, C. Laforsch and G. Gerdts, *Environmental Science &*
- 516 *Technology*, 2017, **51**, 14283-14292.
- 517 40. C. M. Rochman, C. Brookson, J. Bikker, N. Djuric, A. Earn, K. Bucci, S. Athey, A.
- Huntington, H. McIlwraith, K. Munno, H. De Frond, A. Kolomijeca, L. Erdle, J. Grbic,
- M. Bayoumi, S. B. Borrelle, T. Wu, S. Santoro, L. M. Werbowski, X. Zhu, R. K. Giles,
- B. M. Hamilton, C. Thaysen, A. Kaura, N. Klasios, L. Ead, J. Kim, C. Sherlock, A. Ho
- and C. Hung, *Environmental toxicology and chemistry*, 2019, **38**, 703-711.
- 522 41. Z. Tian, H. Zhao, K. T. Peter, M. Gonzalez, J. Wetzel, C. Wu, X. Hu, J. Prat, E.
- Mudrock, R. Hettinger, A. E. Cortina, R. G. Biswas, F. V. C. Kock, R. Soong, A. Jenne,
- B. Du, F. Hou, H. He, R. Lundeen, A. Gilbreath, R. Sutton, N. L. Scholz, J. W. Davis, M.
- 525 C. Dodd, A. Simpson, J. K. McIntyre and E. P. Kolodziej, *Science*, 2021, **371**, 185-189.

- 526 42. V. C. Shruti, F. Pérez-Guevara, I. Elizalde-Martínez and G. Kutralam-Muniasamy,
- *Trends in Environmental Analytical Chemistry*, 2021, **30**, e00123.
- 528 43. S. Ziajahromi, D. Drapper, A. Hornbuckle, L. Rintoul and F. D. L. Leusch, *Science of*
- *The Total Environment*, 2020, **713**, 136356.
- 530 44. S. Herath, D. Hagare, Z. Siddiqui and B. Maheshwari, Environmental Monitoring and
- 531 Assessment, 2022, **194**, 173.
- 532 45. S. Monira, M. A. Bhuiyan, N. Haque, K. Shah, R. Roychand, F. I. Hai and B. K.
- Pramanik, *Process Safety and Environmental Protection*, 2021, **152**, 47-57.
- 534 46. California State Water Resources Control Board, Standard Operating Procedures for
- Extraction and Measurement by Infrared Spectroscopy of Microplastic Particles in
- 536 Drinking Water. Available Online:
- https://www.waterboards.ca.gov/drinking\_water/certlic/drinkingwater/documents/microp
- lastics/mcrplstcs ir.pdf, 2021.
- 539 47. J. E. Ward, S. Zhao, B. A. Holohan, K. M. Mladinich, T. W. Griffin, J. Wozniak and S.
- E. Shumway, *Environmental Science & Technology*, 2019, **53**, 8776-8784.
- 541 48. R. Dris, J. Gasperi, V. Rocher and B. Tassin, Science of The Total Environment, 2018,
- **618**, 157-164.
- 543 49. N. L. Fahrenfeld, G. Arbuckle-Keil, N. Naderi and S. Bartelt-Hunt, *TrAC Trends in*
- 544 *Analytical Chemistry.*, 2019, **112**, 248-254.
- 545 50. J. G. Bokria and S. Schlick, *Polymer*, 2002, **43**, 3239-3246.
- 546 51. G. H. Y. Gao, P. Helm, S. Baker and C. M. Rochman, ACS ES&T Water, 2023, 3, 876-
- 547 884.
- 548 52. N. P. Ivleva, *Chemical Reviews*, 2021, **121**, 11886-11936.